Biophysical Chemistry 137 (2008) 100–104

Contents lists available at ScienceDirect

Biophysical Chemistry

journal homepage: http://www.elsevier.com/locate/biophyschem

# Characterization of the binding of 8-anilinonaphthalene sulfonate to rat class Mu GST M1-1

Nichole Kinsley [a], Yasien Sayed [a], Salerwe Mosebi [a], Richard N. Armstrong [b], Heini W. Dirr [a,*]

[a] Protein Structure-Function Research Unit, School of Molecular and Cell Biology, University of the Wiwatersrand, Johannesburg 2050, South Africa
[b] Department of Biochemistry and Center in Molecular Toxicology, Vanderbilt University School of Medicine, Nashville, Tennessee 37232-0146, USA

ARTICLE INFO

*Article history:*
Received 14 April 2008
Received in revised form 26 July 2008
Accepted 28 July 2008
Available online 5 August 2008

*Keywords:*
ANS
Isothermal titration calorimetry
Ligandin function
Displacement studies
Molecular docking

ABSTRACT

Molecular docking and ANS-displacement experiments indicated that 8-anilinonaphthalene sulfonate (ANS) binds the hydrophobic site (H-site) in the active site of dimeric class Mu rGST M1-1. The naphthalene moiety provides most of the van der Waals contacts at the ANS-binding interface while the anilino group is able to sample different rotamers. The energetics of ANS binding were studied by isothermal titration calorimetry (ITC) over the temperature range of 5–30 °C. Binding is both enthalpically and entropically driven and displays a stoichiometry of one ANS molecule per subunit (or H-site). ANS binding is linked to the uptake of 0.5 protons at pH 6.5. Enthalpy of binding depends linearly upon temperature yielding a $\Delta C_p$ of −80±4 cal $K^{-1}$ $mol^{-1}$ indicating the burial of solvent-exposed nonpolar surface area upon ANS-protein complex formation. While ion-pair interactions between the sulfonate moiety of ANS and protein cationic groups may be significant for other ANS-binding proteins, the binding of ANS to rGST M1-1 is primarily hydrophobic in origin. The binding properties are compared with those of other GSTs and ANS-binding proteins.



## 1. Introduction

In addition to their catalytic functions, cytosolic glutathione transferases (GSTs) are intracellular binding proteins for a wide variety of structurally diverse non-substrate ligands such as bilirubin, haem, steroids, bile salts, carcinogens, dyes and drugs [1]. This ligandin function has implicated these ubiquitous and high capacity binding proteins in the intracellular storage and transport of hydrophobic and amphipathic compounds, many of which inhibit catalytic function (see [2] and references therein). Although their catalytic mechanisms have been investigated extensively (see [3,4] for reviews), relatively little is known about the structural and thermodynamic basis of their ligandin functions.

GSTs are dimers with an active site on each subunit [5]. An active site consists of two adjacent regions; a polar G-site for reduced glutathione and a promiscuous nonpolar H-site for hydrophobic substrates. Crystallographic studies have shed light on the locations and properties of non-substrate binding sites on some GSTs; namely, the H-site of class Pi GST P1-1 [6], the dimer interface of the schistosomal Sj26GST [7] and class Sigma GST [8], and other regions of GSTs to which sulfonate buffer compounds bind [6,9,10]. Other techniques employed to locate the position of and characterize non-substrate binding sites include fluorescence resonance energy transfer [11,12], affinity labelling [13], inhibition kinetics [2,14,15], and isothermal titration calorimetry [16–19].

Very little is known about the ligandin function of class Mu GSTs. In 1975, Ketley et al. [14] reported that 8-anilinonaphthalene sulfonate (ANS), a non-substrate ligand, inhibits competitively class Mu GSTs with respect to the H-site substrate CDNB. ANS, an amphipathic anion, is extensively used to characterize ligand binding sites of proteins. Although generally considered to be a hydrophobic probe, ANS forms ion pairs between its negatively charged sulfonate group and cationic protein groups in most ANS-protein interactions [20–22]. These Coulombic interactions are deemed the primary determinants of ANS binding [23].

In this study, we have employed molecular docking and ligand-displacement experiments as well as isothermal titration calorimetry to identify and characterize the binding sites for ANS on rGST M1-1. Like GSTs from other classes [6,11], ANS binds to the nonpolar H-site, but unlike class Alpha [19] and schistosomal [18] GSTs and other ANS-binding proteins [20–22], hydrophobic interactions govern binding with little contribution from ion pairing involving the sulfonate group of ANS.

*Abbreviations:* ANS, 8-anilinonaphthalene-1-sulphonic acid; FRET, fluorescence-resonance energy transfer; G- and H-sites, glutathione and hydrophobic substrate binding sites; GSH, reduced glutathione; $GSO_3$, glutathione sulfonate; GST, glutathione *S*-transferase; ITC, isothermal titration calorimetry; rGST M1-1, rat glutathione transferase class Mu with two type-1 subunits; TCEP, Tris(2-carboxyethyl)-phosphine.

* Corresponding author.
*E-mail address:* heinrich.dirr@wits.ac.za (H.W. Dirr).

0301-4622/$ – see front matter © 2008 Elsevier B.V. All rights reserved.
doi:10.1016/j.bpc.2008.07.008

## 2. Materials and methods

### 2.1. Materials

8-Anilinonaphthalene sulfonate (ANS), glutathione sulfonate ($GSO_3^-$) and reduced glutathione (GSH) were purchased from Sigma. All other chemicals were of analytical grade. rGST M1-1 was over-expressed using the pET-20b(+) plasmid in *Escherichia coli* BL-21 (DE3) pLys*S* cells [24], and was purified by *S*-hexylglutathione-affinity chromatography. The affinity column was pre-equilibrated with 10 mM Tris–HCl, 200 mM NaCl, 1 mM EDTA, 0.02% sodium azide, pH 7.8, and the bound GST was eluted with 50 mM glycine–NaOH buffer, pH 10 [25]. The protein was buffer-exchanged into 20 mM sodium phosphate, 150 mM NaCl, 1 mM EDTA, 1 mM TCEP and 0.02% sodium azide, pH 6.5. Purity of the protein was confirmed by SDS/PAGE [26] and size-exclusion HPLC. The concentration of dimeric protein was determined spectrophotometrically at 280 nm using a molar absorption coefficient of 81 480 $M^{-1}$ $cm^{-1}$.

### 2.2. Molecular docking

The crystal structures of rGST M1-1 (pdb code 6gst [27]) and ANS (pdb code 2ans [20]) were used for the docking studies. Molegro Virtual Docker [28], which performs flexible ligand docking, was used to predict the interaction of ANS with rGST M1-1. PyMol [29] was used for the visualization of the docked ANS conformations.

### 2.3. ANS displacement studies

The displacement of ANS bound to rGST M1-1 by various active site ligands was measured by monitoring the fluorescence of ANS at 483 nm (excitation at 390 nm) [19]. A solution of 2 μM rGST M1-1 and 200 μM ANS was titrated with increasing concentrations of GSH, $GSO_3^-$, and ethacrynic acid. All experiments were carried out in 20 mM sodium phosphate, 150 mM NaCl, 1 mM EDTA, 1 mM TCEP and 0.02% sodium azide, pH 6.5. The concentrations of ligand stock solutions were 5 mM GSH, 1.5 mM $GSO_3^-$ and 6 mM ethacrynic acid. Data were corrected for blanks (no protein) and for dilution (<10%).

### 2.4. Isothermal titration calorimetry

Calorimetric studies with a VP-ITC calorimeter from Microcal (Northampton, MA, U.S.A.) and data analysis were performed as described [16,38]. Protein was extensively dialysed against 20 mM sodium phosphate buffer (pH 6.5) containing 150 mM NaCl, 1 mM EDTA, 1 mM TCEP and 0.02% sodium azide, and used at a subunit concentration of 70 μM. ANS was prepared as a stock of 3.3 mM in the final dialysate buffer. Total observed heats were corrected for heats of dilution, and the corrected data analysed by non-linear regression with Origin 5 (MicroCal). The resulting fit of the data gives observed apparent dissociation constant, $K_d$, the enthalpy of binding, $\Delta H^o_{obs}$, and the stoichiometry of the reaction per subunit, *N*. The Gibbs free energy and binding entropy were calculated using the conventional relations $\Delta G^\circ_{obs} = RT\ln(K_d)$ and $T\Delta S^\circ_{obs} = \Delta H^o_{obs} - \Delta G^\circ_{obs}$.

To determine whether the observed enthalpy of ANS binding to rGST M1-1 is coupled to protonation effects, titration experiments were performed at 25 °C and pH 6.5 in buffers with different ionization enthalpies [54]. The buffers used were phosphate ($\Delta H_{ion}$ = 1.22 kcal $mol^{-1}$), Pipes ($\Delta H_{ion}$ = 2.74 kcal $mol^{-1}$), Mes ($\Delta H_{ion}$ = 3.71 kcal $mol^{-1}$), Mops ($\Delta H_{ion}$ = 5.22 kcal $mol^{-1}$) and imidazole ($\Delta H_{ion}$ = 8.75 kcal $mol^{-1}$) [55].

## 3. Results and discussion

Although the structures of GST•ANS complexes have not been elucidated, molecular docking and ligand-displacement experiments indicate that ANS binds at the H-site of rGST M1-1. The molecular model of the complex, as predicted by Molegro Virtual Docker [28], is shown in Fig. 1. Whereas ANS has been reported to affect the conformation of some proteins [30], our docking experiments were performed with the assumption that ANS binding does not alter the structure of rGST M1-1. This assumption is supported by the findings that show the anionic dye not to impact the conformational stability of GSTs ([15,18,31], R. Ohlemeyer, W.H. Kaplan and Dirr, unpublished results). The hydrophobic anilino and naphthyl rings of ANS are within 4 Å of Tyr6, Trp7, Val9, Gly11, Met34, Ile111, Tyr115, Ile207, Phe208, Ser209 and Leu211. While the naphthalene ring system is buried within the H-site pocket, the anilino ring is exposed and dynamic and samples different locations between Met108 in helix 4 and Tyr 115 in the bend between helices 4 and 5 (Fig. 1B). The H-site was previously identified in the crystal structures of rGST M1-1 complexed with various ligands [32]. The negatively charged sulfonate group of ANS is also exposed and points towards the side chain of Arg42. The solvent accessible and flexible guanidinium group of Arg42 is a good candidate for interacting electrostatically with ANS. Ion pairing between the sulfonate of ANS and an arginine side chain is also observed for hGST A1-1 [19] and other ANS-binding proteins [20–22]. The hydrophobic nature of the class Mu binding site for ANS is consistent with the enhanced emission intensity and blue shifted (from 530 nm to 495 nm) fluorescence spectrum of the dye when bound to rGST M1-1 [33]. These spectral features are generally attributed to the hydrophobicity of an internal binding site and restricted mobility of ANS (other ANS-binding proteins [20–22]). The spectroscopic data, however, suggests that the class Mu ANS-binding

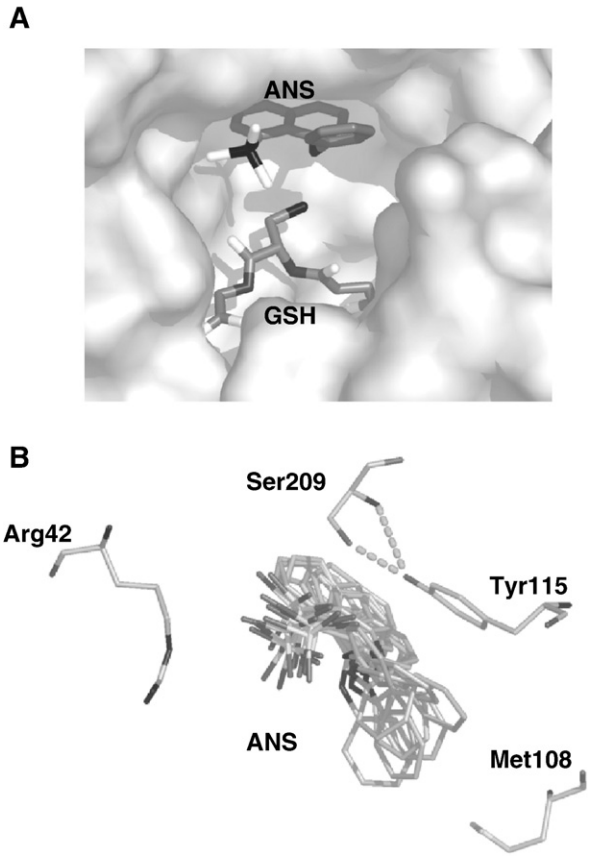


**Fig. 1.** Simulated binding of ANS to rGST M1-1. Molegro Virtual Docker (A) Stick representations of GSH bound at the G-site (pdb 6gst), and ANS bound at the H-site as simulated by Molegro Virtual Docker [28]. rGST M1-1 is represented by the molecular surface. (B) Binding modes of ANS displaying different conformations of the ligand. The side-chains of Arg42 near the sulfonate group of ANS, Met108, Tyr115 and Ser209 are shown. The broken line represents hydrogen bonding between Tyr115 and Ser209.

site is less hydrophobic (smaller blue shift) and more solvent exposed (lower enhanced intensity) than the class Alpha site. The helix that covers the H-site in the class Alpha structure is not present in class Mu GST making its H-site more exposed to solvent and therefore, ANS at this site is more prone to fluorescence quenching by water.

That ANS binds at the H-site of rGST M1-1 is demonstrated by its displacement by ethacrynic acid, an H-site ligand [25,34,35] (Fig. 2). This is supported by the finding that ANS inhibits rat class Mu GSTs competitively with respect to the H-site substrate CDNB [14]. Interestingly, $GSO_3^-$ but not GSH, also displaces ANS (Fig. 2). While both tripeptides are G-site ligands, the displacement of ANS by $GSO_3^-$

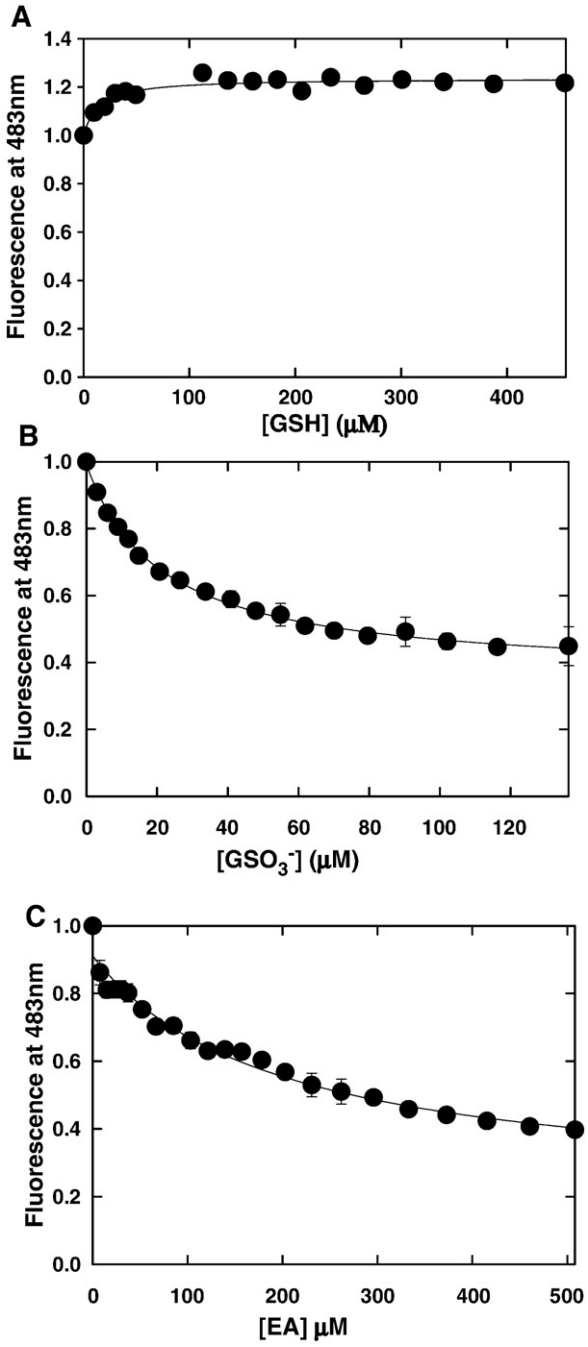


**Fig. 2.** Displacement of ANS bound to rGST M1-1 by (A) GSH, (B) $GSO_3^-$ and (C) ethacrynic acid. Samples, consisting of 200 μM ANS and 2 μM protein, were titrated with the active site ligands and the fluorescence of bound ANS followed at 483 nm (excitation at 390 nm).

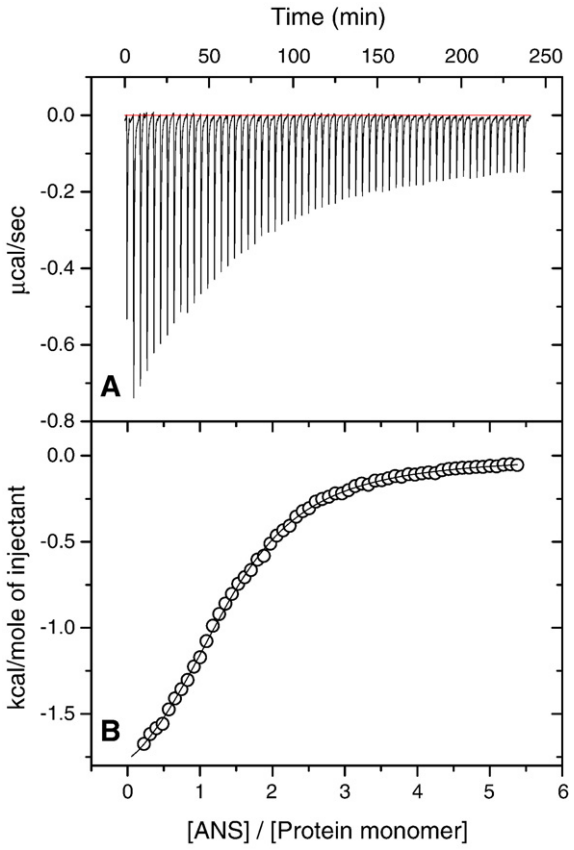


**Fig. 3.** Representative calorimetric profile of the binding of ANS to rGST M1-1 (25 °C). The protein (subunit concentration of 70 μM) was titrated with increasing amounts of ANS from a stock solution of 3.3 mM. Panel A shows the raw exothermic heats associated with ANS binding. Panel B shows the integrated data in (A) after correction for heats of dilution. The solid line represents the non-linear least squares fit to the data according to a single binding site per monomer model.

can be explained by the intrusion of the larger, negatively charged sulfonate group of $GSO_3^-$ into the adjacent H-site resulting in steric and coulombic repulsion between the sulfonate groups. The close approach of the groups is evident in our structural model (Fig. 1) and the crystal structures of GST•$GSO_3^-$ complexes [36,37]. Simply put, the binding space for ANS and $GSO_3^-$ would overlap resulting in displacement.

The energetics of ANS binding to the H-site of rGST M1-1 was investigated by ITC over the temperature range of 5–30 °C. The interaction between ANS and rGST M1-1 is exothermic (Fig. 3A) and the binding isotherm follows a model for a single binding site per subunit (Fig. 3B). A binding stoichiometry of one molecule of ANS at this site was observed for the temperature range used. Whereas class Alpha hGST A1-1 also binds a single molecule of ANS at each H-site [16,19,38], the schistosomal Sj26GST displays a binding stoichiometry of one ANS per dimer at a site that is distinct from the active sites of the enzyme [18]. Whether this site is the same as that observed for the drug praziquantel at the dimer interface of Sj26GST [7], remains to be determined. The affinity of rGST M1-1 for ANS ($K_d$ = 27 ± 1.2 μM) is slightly higher than that of hGST A1-1 ($K_d$ = 65 μM; [16]) but is 13-fold tighter than that of Sj26GST ($K_d$ = 357 μM; [18]). The free energy of rGST M1-1•ANS complex formation remains relatively constant throughout the temperature range employed (Fig. 4). This is due to the increasingly negative enthalpy compensating for the decreasingly positive entropy. Enthalpy–entropy compensation [39] is characteristic of weak intermolecular interactions [40] and solvent reorganization accompanying the formation of protein–ligand complexes

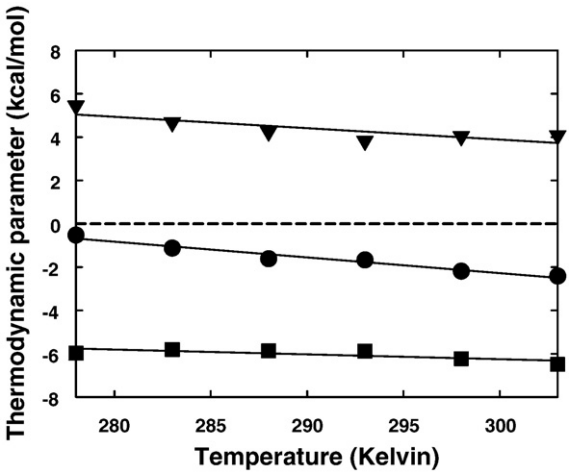


**Fig. 4.** Temperature dependence of the thermodynamic parameters for the binding of ANS to rGST M1-1. The solid lines represent linear regressions to the experimental data for $\Delta H^{o}_{obs}$ (●; $R^2$=0.961), $T\Delta S^{o}_{obs}$ (▲; $R^2$=0.686) and $\Delta G^{o}_{obs}$ (■; $R^2$=0.603). The heat capacity change associated with ANS binding was determined from the slope of $\Delta H$ versus temperature.

[39,41–43]. The relationship between enthalpy and entropy is linear and equal to unity (data not shown), indicating complete compensation and a single interaction mechanism [41,43]. At 25 °C, rGST M1-1•ANS complex formation is both enthalpically ($\Delta H^{o}_{obs}$=−2.2±0.02 kcal mol$^{-1}$) and entropically ($T\Delta S^{o}_{obs}$=4.04±0.02 kcal mol$^{-1}$) driven. The situation is different for both hGST A1-1 and Sj26GST for which ANS binding is enthalpically favourable ($\Delta H^{o}_{obs}$ −7.3 kcal mol$^{-1}$ and −12.5 kcal mol$^{-1}$, respectively) but is entropically unfavourable ($T\Delta S^{o}_{obs}$=−1.7 kcal mol$^{-1}$ and −7.7 kcal mol$^{-1}$, respectively). Experiments at 25 °C using buffers with different ionization enthalpies, $\Delta H_{ion}$, indicate that 0.5 protons were taken up during the binding of ANS to rGST M1-1 (data not shown). The intrinsic binding enthalpy, $\Delta H^{o}_{bind}$, taking the number of protons exchanged, $n^{+}_{H}$, into account was calculated as −2.81±0.18 kcal mol$^{-1}$ from the equation [54]:

$$\Delta H^{o}_{obs} = \Delta H^{o}_{bind} + n^{+}_{H}\Delta H^{o}_{ion}$$

The extent to which proton exchange is linked to the binding of ANS to other GSTs is not known. The positive entropy change for the class Mu GST indicates a net favourable entropy change of solvation, in that restrained waters hydrating nonpolar surfaces of the H-site and ANS are released into bulk solvent upon complex formation [44]. Further, desolvation of the interacting surfaces compensates for binding-induced losses in the conformational entropy of the protein and the dye. It is likely that the configurational entropy lost upon ANS binding to rGST M1-1 is less than that for both hGST A1-1 and Sj26GST. ANS is relatively constrained and has only two degrees of freedom (about the dihedral angle of the anilino moiety with respect to the naphthyl ring and the torsion angle by which the phenyl ring is rotated about the N-C1' axis) (see [16]). Molegro Virtual Docker simulations of the ANS-rGST M1-1 complex show that, while the naphthalene moiety remains positioned in the hydrophobic pocket of the H-site, the anilino group is dynamic (Fig. 1B). It is possible that, unlike the Alpha and Sj26GST class H-sites, the class Mu site does not effectively restrict ANS. It is also unlikely that ANS binding interferes with the hydrogen bond interactions between Tyr 115 and Ser 209 that inhibit the segmental dynamics of the C-terminal tail and helices 4 and 5 [32,45,46] (see Fig. 1B). Regarding the entropically unfavourable binding of ANS to hGST A1-1, its C-terminal tail is highly dynamic and delocalized in the apo protein [25,47]. However, when ligands bind the H-site, the tail forms a helix that covers the active site [25,47,48], an event that likely contributes towards the unfavourable entropy of ANS binding [19]. Mutants in which helix 9 remains delocalized in ANS-complexed protein display an interaction that is both enthalpically and entropically favourable [49].

The linear temperature dependence of enthalpy (Fig. 4) yields a heat capacity change, $\Delta C_p$, of −80±4 cal K$^{-1}$ mol$^{-1}$ for the rGST M1-1•ANS interaction. Inasmuch as a change in heat capacity originates primarily from the changes in the hydration of molecular surface areas [50], the larger negative $\Delta C_p$ values of −201 cal K$^{-1}$ mol$^{-1}$ and −295 cal K$^{-1}$ mol$^{-1}$ for hGST A1-1 [16] and Sj26GST [18], respectively, indicate that the binding of ANS to these proteins is accompanied by the burial of more hydrophobic surface area [51]. Two lipid-binding proteins, IFABP and ALBP, also display larger negative $\Delta C_p$ values (−282 cal K$^{-1}$ mol$^{-1}$ [52] and −220 cal K$^{-1}$ mol$^{-1}$ [20], respectively) upon binding ANS as compared to that for rGST M1-1. The burial of less solvent-exposed nonpolar surface area during the formation of the rGST M1-1•ANS complex appears to be consistent with the dye's greater exposure to solvent than when bound to the less exposed internal sites of hGST A1-1 [16] and ALBP [20]. Enthalpic van der Waals contacts formed between the anilinonaphthalene moiety and the H-site most likely contribute more significantly towards binding energy than potential electrostatic interactions since the latter have been reported not to account for the micromolar binding affinities for ANS binding [16,20,52]. The smaller negative $\Delta C_p$ for the rGST M1-1•ANS interaction might be due to the high mobility of ANS bound to rGST M1-1, as suggested by the docking results, which would result in a smaller reduction in enthalpy fluctuations upon binding.

The hydrophobic effect is most likely the principal driving force behind formation of the rGST M1-1•ANS complex, but due to the presence of a charged sulfonate and potential electrostatic effects, it may not be a conventional hydrophobic interaction [53]. This is contrary to the findings of Matulis and Lovrien [23] who claim that the binding of ANS to proteins is primarily dependent on ion-pair formation where the sulfonate group is the major binding determinant and that the anilinonaphthalene moiety only serves to reinforce binding.

## Acknowledgements

This work was supported by the University of the Witwatersrand, the South African National Research Foundation Grant 205359, the South African Research Chairs Initiative of the Department of Science and Technology and National Research Foundation Grant 64788, the Fogarty International Research Collaboration Award TW000779, and Grants R01 GM030910, and P30 ES000267 from the National Institutes of Health. Any opinion, findings and conclusions or recommendations expressed in this material are those of the author(s) and therefore the NRF and DST do not accept any liability with regard thereto.

## References

[1] G. Litwack, B. Ketterer, I.M. Arias, Ligandin: a hepatic protein which binds steroids, bilirubin, carcinogens and a number of exogenous organic anions, Nature 234 (1971) 466–467.
[2] R.P. Lyon, W.M. Atkins, Kinetic characterization of native and cysteine 112-modified glutathione *S*-transferase A1-1: reassessment of nonsubstrate ligand binding, Biochemistry 41 (2002) 10920–10927.
[3] R.N. Armstrong, Glutathione S-transferases: reaction mechanism, structure, and function, Chem. Res. Toxicol. 4 (1991) 131–140.
[4] R.N. Armstrong, Structure, catalytic mechanism, and evolution of the glutathione transferases, Chem. Res. Toxicol. 10 (1997) 2–18.
[5] H. Dirr, P. Reinemer, R. Huber, X-ray crystal structures of cytosolic glutathione *S*-transferases. Implications for protein architecture, substrate recognition and catalytic function, Eur. J. Biochem. 220 (1994) 645–661.
[6] A.J. Oakley, M. Lo Bello, M. Nuccetelli, A.P. Mazzetti, M.W. Parker, The ligandin (non-substrate) binding site of human Pi class glutathione transferase is located in the electrophile binding site (H-site), J. Mol. Biol. 291 (1999) 913–926.
[7] M.A. McTigue, D.R. Williams, J.A. Tainer, Crystal structures of a schistosomal drug and vaccine target: glutathione *S*-transferase from *Schistosoma japonica* and its complex with the leading antischistosomal drug praziquantel, J. Mol. Biol. 246 (1995) 21–27.
[8] X. Ji, E.C. von Rosenvinge, W.W. Johnson, R.N. Armstrong, G. Gilliland, Location of a potential transport binding site in a sigma class glutathione transferase by X-ray crystallography, Proc. Natl. Acad. Sci. U. S. A. 93 (1996) 8208–8213.

[9] L. Prade, R. Huber, T.H. Manoharan, W.E. Fahl, W. Reuter, Structures of class pi glutathione *S*-transferase from human placenta in complex with substrate, transition-state analogue and inhibitor, Structure 5 (1997) 1287–1295.
[10] X. Ji, M. Tordova, R. O'Donnell, J.F. Parsons, J.B. Hayden, G.L. Gilliland, P. Zimniak, Structure and function of the xenobiotic substrate-binding site and location of a potential non-substrate-binding site in a class pi glutathione *S*-transferase, Biochemistry 36 (1997) 9690–9702.
[11] N. Sluis-Cremer, N.N. Naidoo, W.H. Kaplan, T.H. Manoharan, W.E. Fahl, H.W. Dirr, Determination of a binding site for a non-substrate ligand in mammalian cytosolic glutathione *S*-transferases by means of fluorescence-resonance energy transfer, Eur. J. Biochem. 241 (1996) 484–488.
[12] N. Sluis-Cremer, L.A. Wallace, J. Burke, J.M. Stevens, H. Dirr, Aflatoxin B1 and sulphobromophthalein binding to the dimeric human *S*-transerase A1-1: a fluorescence spectroscopic analysis, Eur. J. Biochem. 257 (1998) 434–442.
[13] J.J. Barycki, R.F. Colman, Identification of the nonsubstrate steroid binding site of rat liver glutathione *S*-transferase, isozyme 1-1, by the steroid affinity label, 3beta-(iodoacetoxy)dehydroisoandrosterone, Arch. Biochem. Biophys. 345 (1997) 16–31.
[14] J.N. Ketley, W.H. Habig, W.B. Jakoby, Binding of nonsubstrate ligands to the glutathione *S*-transferases, J. Biol. Chem. 250 (1975) 8670–8673.
[15] P. Bico, J. Erhardt, W. Kaplan, H. Dirr, Porcine class pi glutathione *S*-transferase: anionic ligand binding and conformational analysis, Biochim. Biophys. Acta 1247 (1995) 225–230.
[16] Y. Sayed, J.A. Hornby, M. Lopez, H. Dirr, Thermodynamics of the ligandin function of human class Alpha glutathione transferase A1-1: energetics of organic anion ligand binding, Biochem. J. 363 (2002) 341–346.
[17] D. Kolobe, Y. Sayed, H.W. Dirr, Characterization of bromosulphophthalein binding to human glutathione *S*-transferase A1-1: thermodynamics and inhibition kinetics, Biochem. J. 382 (2004) 703–709.
[18] Z. Yassin, E. Ortiz-Salmeron, F. Garcia-Maroto, C. Baron, L. Garcia-Fuentes, Implications of the ligandin binding site on the binding of non-substrate ligands to Schistosoma japonicum-glutathione transferase, Biochim. Biophys. Acta 1698 (2004) 227–237.
[19] H.W. Dirr, T. Little, D.C. Kuhnert, Y. Sayed, A conserved N-capping motif contributes significantly to the stabilisation and dynamics of the C-terminal region of class alpha glutathione transferases, J. Biol. Chem. 280 (2005) 19480–19487.
[20] J.J. Ory, L.J. Banaszak, Studies of the ligand binding reaction of adipocyte lipid binding protein using the fluorescent probe 1, 8-anilinonaphthalene-8-sulfonate, Biophys. J. 77 (1999) 1107–1116.
[21] E. Schonbrunn, S. Eschenburg, K. Luger, W. Kabsch, N. Amrhein, Structural basis for the interaction of the fluorescence probe 8-anilino-1-naphthalene sulfonate (ANS) with the antibiotic target MurA, Proc. Natl. Acad. Sci. U. S. A. 97 (2000) 6345–6349.
[22] A. Lartigue, A. Gruez, S. Spinelli, S. Riviere, R. Brossut, M. Tegoni, C. Cambillau, The crystal structure of a cockroach pheremone-binding protein suggests a new ligand binding and release mechanism, J. Biol. Chem. 278 (2003) 30213–30218.
[23] D. Matulis, R. Lovrien, 1-anilino-8-napthalene sulfonate anion-protein binding depends primarily on ion pair formation, Biophys. J. 74 (1998) 422–429.
[24] P.H. Zhang, R.N. Armstrong, Construction, expression, and preliminary characterization of chimeric class mu glutathione *S*-transferases with altered catalytic properties, Biopolymers 29 (1990) 159–169.
[25] A.D. Cameron, I. Sinning, G. L'Hermite, B. Olin, P.G. Board, B. Mannervik, T.A. Jones, Structural analysis of human alpha-class glutathione transferase A1-1 in the apo-form and in complexes with ethacrynic acid and its glutathione conjugate, Structure 3 (1995) 717–727.
[26] U.K. Laemmli, Cleavage of structural proteins during the assembly of the head of bacteriophage T4, Nature 227 (1970) 680–685.
[27] G. Xiao, S. Liu, X. Ji, W.W. Johnson, J. Chen, J.F. Parsons, W.J. Stevens, G.L. Gilliland, R.N. Armstrong, First-sphere and second-sphere electrostatic effects in the active site of a class mu gluthathione transferase, Biochemistry 35 (1996) 4753–4765.
[28] R. Thomsen, M.H. Christensen, MolDock: a new technique for high-accuracy molecular docking, J. Med. Chem. 49 (2006) 3315–3321.
[29] W.L. Delano, The PyMOL Molecular Graphics System, DeLano Scientific, San Carlos CA, USA, 2004 http://pymol.sourceforge.net/.
[30] M.S. Celej, S.A. Dassie, E. Freire, M.L. Bianconi, G.D. Fidelio, Ligand-induced thermostability in proteins: thermodynamic analysis of ANS-albumin interaction, Biochim. Biophys. Acta 1750 (2005) 122–133.
[31] L.A. Wallace, H.W. Dirr, Folding and assembly of dimeric human glutathione transferase A1-1, Biochemistry 38 (1999) 16686–16694.
[32] X. Ji, W.W. Johnson, M.A. Sesay, L. Dickert, S.M. Prasad, H.L. Ammon, R.N. Armstrong, G.L. Gilliland, Structure and function of the xenobiotic substrate binding site of a glutathione *S*-transferase as revealed by X-ray crystallographic analysis of product complexes with the diastereomers of 9-(*S*-glutathionyl)-10-hydroxy-9,10-dihydrophenanthrene, Biochemistry 33 (1994) 1043–1052.
[33] J.A.T. Hornby, J. Luo, J.M. Stevens, L.A. Wallace, W. Kaplan, R.N. Armstrong, H. Dirr, Equilibrium folding of dimeric class mu glutathione transferases involves a stable monomeric intermediate, Biochemistry 39 (2000) 12336–12344.
[34] B. Mannervik, U.H. Danielson, Glutathione transferases — structure and catalytic activity, CRC Crit. Rev. Biochem. 23 (1988) 283–337.
[35] A.J. Oakley, J. Rossjohn, M. Lo Bello, A.M. Caccuri, G. Federici, M.W. Parker, The three-dimensional structure of the human Pi class glutathione transferase P1-1 in complex with the inhibitor ethacrynic acid and its glutathione conjugate, Biochemistry 36 (1997) 576–585.
[36] P. Reinemer, H.W. Dirr, R. Ladenstein, J. Schaffer, O. Gallay, R. Huber, The three-dimensional structure of class pi glutathione *S*-transferase in complex with glutathione sulfonate at 2.3 A resolution, Embo. J. 10 (1991) 1997–2005.
[37] H. Dirr, P. Reinemer, R. Huber, Refined crystal structure of porcine class Pi glutathione *S*-transferase (pGST P1-1) at 2.1 A resolution, J. Mol. Biol. 243 (1994) 72–92.
[38] S. Mosebi, Y. Sayed, J. Burke, H.W. Dirr, Residue 219 impacts on the dynamics of the C-terminal region in glutathione transferase A1-1: implications for stability and catalytic and ligandin functions, Biochemistry 42 (2003) 15326–15332.
[39] R. Lumry, S. Rajender, Enthalpy-entropy compensation phenomena in water solutions of proteins and small molecules: a ubiquitous property of water. Biopolymers 9 (1970) 1125–1227.
[40] J.D. Dunitz, The entropic cost of bound water in crystals and biomolecules, Science 264 (1994) 670.
[41] C.P. Swaminathan, N. Surolia, A. Surolia, Role of water in the specific binding of mannose and mannooligosaccharides to concanavalin A, J. Am. Chem. Soc. 120 (1998) 5153–5159.
[42] R.U. Lemieux, How water provides the impetus for molecular recognition in aqueous solution, Acc. Chem. Res. 29 (1996) 373–380.
[43] J.E. Leffler, E. Grunwald, Rates and Equilibria of Organic Reactions, John Wiley and Sons, Inc., New York, 1963.
[44] J.M. Sturtevant, Heat capacity and entropy changes in processes involving proteins, Proc. Natl. Acad. Sci. U. S. A. 74 (1977) 2236–2240.
[45] W.W. Johnson, S. Liu, X. Ji, G.L. Gilliland, R.N. Armstrong, Tyrosine 115 participates both in chemical and physical steps of the catalytic mechanism of a glutathione *S*-transferase, J. Biol. Chem. 268 (1993) 11508–11511.
[46] S.G. Codreanu, J.E. Ladner, G. Xiao, N.V. Stourman, D.L. Hachey, G.L. Gilliland, R.N. Armstrong, Local protein dynamics and catalysis: detection of segmental motion associated with rate-limiting product release by a glutathione transferase, Biochemistry 41 (2002) 15161–15172.
[47] M. Le, G.E. Means, A procedure for the determination of monothiols in the presence of dithiothreitol — an improved assay for the reduction of disulfides, Anal. Biochem. 229 (1995) 264–271.
[48] I. Sinning, G.J. Kleywegt, S.W. Cowan, P. Reinemer, H.W. Dirr, R. Huber, G.L. Gilliland, R.N. Armstrong, X. Ji, P.G. Board, B. Olin, B. Mannervik, T.A. Jones, Structure determination and refinement of human alpha class glutathione transferase A1-1, and a comparison with the Mu and Pi class enzymes, J. Mol. Biol. 232 (1993) 192–212.
[49] D.C. Kuhnert, Y. Sayed, S. Mosebi, M. Sayed, T. Sewell, H.W. Dirr, Tertiary interactions stabilise the c-terminal region of human glutathione transferase A1-1: a crystallographic and calorimetric study, J. Mol. Biol. 349 (2005) 825–838.
[50] E. Freire, Thermodynamics of protein folding and molecular recognition. Pure Appl. Chem. 69 (1997) 2253–2261.
[51] V.V. Loladze, D.N. Ermolenko, G.I. Makhatadze, Heat capacity changes upon burial of polar and nonpolar groups in proteins, Protein Sci. 10 (2001) 1343–1352.
[52] W.R. Kirk, E. Kurian, F.G. Prendergast, Characterization of the sources of protein–ligand affinity: 1-sulfonato-8-(1')anilinonaphthalene binding to intestinal fatty acid binding protein, Biophys. J. 70 (1996) 69–83.
[53] E. Kurian, W.R. Kirk, F.G. Prendergast, Affinity of fatty acid for (r)rat intestinal fatty acid binding protein: further examination, Biochemistry 35 (1996) 3865–3874.
[54] B.M. Baker, K.P. Murphy, Evaluation of linked protonation effects in protein binding reactions using isothermal titration calorimetry, Biophys. J. 71 (1996) 2049–2055.
[55] H. Fukada, K. Takahashi, Enthalpy and heat capacity changes for the proton dissociation of various buffer components in 0.1 M potassium chloride, Proteins 33 (1998) 159–166.